PCCP

Direct detection of polar structure formation in helium nanodroplets by beam deflection measurements

Journal:	*Physical Chemistry Chemical Physics*
Manuscript ID	CP-ART-08-2019-004322.R1
Article Type:	Paper
Date Submitted by the Author:	01-Sep-2019

Complete List of Authors:	Niman, John; University of Southern California, Physics and Astronomy Kamerin, Benjamin; University of Southern California, Physics and Astronomy Kranabetter, Lorenz; University Innsbruck, Institut für Ionenphysik und Angewandte Physik Merthe, Daniel; University of Southern California, Physics and Astronomy Suchan, Jiří; University of Chemistry and Technology, Prague, Physical Chemistry Slavicek, Petr; University of Chemistry and Technology, Prague, Physical Chemistry Kresin, Vitaly; University of Southern California, Physics and Astronomy

Direct detection of polar structure formation in helium nanodroplets by beam deflection measurements

John W. Niman,[a] Benjamin S. Kamerin,[a] Lorenz Kranabetter,[b] Daniel J. Merthe,[a†]
Jiří Suchan,[c] Petr Slavíček,*[cd] Vitaly V. Kresin*[a]

[a] *Department of Physics and Astronomy, University of Southern California, Los Angeles, CA 90089-0484, USA*

[b] *Institut für Ionenphysik und Angewandte Physik, Universität Innsbruck, Technikerstr. 25, A-6020 Innsbruck, Austria*

[c] *Department of Physical Chemistry, University of Chemistry and Technology, Technická 5, Prague 6, Czech Republic*

[d] *J. Heyrovský Institute of Physical Chemistry v.v.i., The Czech Academy of Sciences, Dolejškova 3, 18223 Prague, Czech Republic*

[†] *Present address: Modern Electron, Bellevue, WA 98007, USA.*

Abstract

Long-range intermolecular forces are able to steer polar molecules submerged in superfluid helium nanodroplets into highly polar metastable configurations. We demonstrate that the presence of such special structures can be identified, in a direct and determinative way, by electrostatic deflection of the doped nanodroplet beam. The measurement also establishes the structures' electric dipole moments. In consequence, the introduced approach is complementary to spectroscopic studies of low-temperature molecular assembly reactions. It is enabled by the fact that within the cold superfluid matrix the molecular dipoles become nearly completely oriented by the applied electric field. As a result, the massive (tens of thousands of helium atoms) nanodroplets undergo significant deflections. The method is illustrated here by an application to dimers and trimers of dimethyl sulfoxide (DMSO) molecules. We interpret the experimental results with ab initio theory, mapping the potential energy surface of DMSO complexes and simulating their low temperature aggregation dynamics.

1. Introduction

Long-range intermolecular forces play an essential role in reactions at sub-Kelvin temperatures (see, e.g., the reviews in refs 1-4). For example, long-range interactions between polar molecules embedded in helium nanodroplets often dominate the outcome of their assembly reactions. This is facilitated by the low internal temperature (370 mK) of the nanodroplet medium as well as by its superfluidity.[5] As a result, molecular reorientation and intermolecular reactions within nanodroplets are not perturbed by inhomogeneities present in other low-temperature surface and matrix isolation environments, making these "nano-cryo-traps" excellent hosts for exploring the physics and chemistry of cold molecular systems.[6]

A landmark demonstration of the action of long-range forces was furnished by experiments on HCN molecules sequentially picked up by a He nanodroplet beam.[7] These linear molecules were guided by dipole-dipole forces to self-assemble into long chains aligned head-to-tail inside the nanodroplet. HCCCN was found to behave similarly.[8] These chains rank among the most polar molecular systems ever observed in a molecular beam. In an "ordinary" environment thermal motion would drive them out of this type of metastable configuration, but within a very cold and inert liquid helium droplet they become long-lived. Data on formic acid,[9] imidazole,[10] and acetic acid[11,12] dimers suggested an analogous alignment mechanism.

However, such an outcome is not universal in nanodroplet embedding. For example, two HCl molecules arrange themselves nearly at a right angle to each other[13,14] while water clusters form cyclic structures.[15] The "decision" by polar molecules how to orient themselves upon approach depends on the strength of their dipoles, on their responsiveness to the mutually reorienting torques (i.e., their rotational constants and their accessible rotational quantum states), and on the directionality and flexibility of their bond formation. That is to say, the outcome depends on the shape of the intermolecular potential energy surface and on

the barrier heights encountered on the path to the final configuration.

It is therefore interesting and informative to establish whether a molecular formation within a nanodroplet can reach its global energy minimum or finds itself trapped in a polar metastable state. However, often this is not a straightforward determination. The studies cited above based their conclusions on the interpretation of dopant infrared spectra or on inference from electron attachment mass spectrometry. Such assignments grow more difficult and less definitive with increasing size and/or complexity of the embedded molecules and their assemblies.

In this work we describe a measurement which *directly* establishes the polarity of a molecular assembly, as well as determines its dipole moment. It makes use of electrostatic deflection of the doped nanodroplet beam.[16,17]

The technique is based on the fact that polar structures embedded within the superfluid matrix can be made nearly fully oriented by an external static electric field[18] and consequently experience an extremely large deflecting force from the field's gradient. Such a high degree of orientation is unattainable for bare polyatomic complexes in a molecular beam. Whereas some relatively small and light molecules reach rotational temperatures T_{rot} below 1 K with the use of seeded supersonic expansions and exhibit large deflections (see, e.g., refs 19,20), this becomes impractical for heavier systems.

For the purpose of an estimate, consider the classical Langevin function for the orientation of a molecular rotor in an external field $E\hat{z}$: $\bar{p}_z / p_0 = \left[\coth x - 1/x\right]$. This is a good approximation[21,22] for $k_B T_{rot} >> B$. Here p_0 is the molecule's dipole moment, $\bar{p}_z$ is the average projection of this dipole on the field axis, $x \equiv p_0 E / k_B T_{rot}$, and B is the rotational constant. For T_{rot} above a few K and practical electric field strengths, the ratio x remains

small even for dipole moments of several Debye (D), and in this limit $\bar{p}_z / p_0 \approx x/3 = 1$. Therefore it is only when the rotational temperature becomes very low, as enabled in the present case by helium nanodroplet isolation, that the orientation can approach saturation $(\bar{p}_z \to p_0)$. This effect has been taken advantage of in landmark experiments using pendular-state spectroscopy.[18]

If the external electric field which orients the nanodroplet-submerged dipoles is designed also to have a collinear strong gradient, then these dipoles will experience such a strong side-ways force $F_z = p_z (\partial E/\partial z)$ that the massive doped droplets, comprised of tens of thousands of helium atoms, will be significantly deflected in their entirety. Thus, our procedure involves comparing the deflection profile of a singly-doped nanodroplet beam with that of a beam composed of multiply-doped nanodroplets. If, for example, the droplets containing two (or three, etc.) molecules show negligible deflection, we can immediately conclude that the dimer (trimer, etc.) has settled into a nonpolar configuration. A strongly deflected profile, on the other hand, immediately attests to the formation of a polar structure, and the magnitude of the deflection translates into the magnitude of this formation's total dipole moment.

This is a conveniently unambiguous measurement applicable to a wide range of molecules, from diatomic to polyatomic (including biological). Practically any molecular species that can be brought into the vapor phase with a pressure of only 10^{-6}-10^{-4} mbar can be picked up by the nanodroplet beam and thermalized within the inert viscosity-free medium. The thermalization proceeds by evaporative cooling: the molecules' translational and internal energies are transferred to the superfluid matrix which has a very high thermal conductivity, and released via evaporation of surface helium atoms, promptly bringing the nanodroplet back to the original temperature.[5]

Here we apply the deflection method to monomers, dimers and trimers of the dimethyl

sulfoxide molecule ("DMSO," $(CH_3)_2SO$, molecular mass 78 Da). The molecule is nearly an oblate symmetric top, with rotational constants of[23,24] 0.235 cm^{-1}, 0.231 cm^{-1}, and 0.141 cm^{-1} and its total dipole moment is[25] p=4.0 D. The measurement clearly reveals the presence of highly polar dimers and trimers, i.e., the formation of metastable polar configurations abetted by the cryogenic nanodroplet environment. To our knowledge, this is the first direct non-spectroscopic identification of such a cold polar molecular assembly.

2. Results and Discussion

2.1 Deflection profiles. The experimental setup has been described in detail elsewhere.[16,17,26] A nanodroplet beam is formed by cold nozzle expansion of pure helium gas. It passes first through a pick-up cell filled with DMSO vapor, and then between two high-voltage electrodes which create an electric field and a collinear field gradient directed perpendicular to the beam axis. Downstream, the beam enters through a slit into an electron-impact ionizer, and the intensities of the resulting molecular ions are recorded by a quadrupole mass spectrometer in synchronization with a beam chopper. The deflection induced by the electric field is determined by comparing the beam's "field-on" and "field-off" spatial profiles which are mapped out by translating the detector chamber, with its entrance slit, on a precision linear stage.

Molecules are picked up by helium nanodroplets via successive collisions in a Poisson process.[5] Therefore it is important to correlate measured beam deflections with the specific number of molecules embedded in the droplet. Dopants within nanodroplets are ionized indirectly via charge transfer to He^+ produced by electron bombardment; this transfer is a highly exothermic process which can cause fragmentation.[27] Consequently, when mapping out the deflection profile of a dopant ion peak in the mass spectrum, we need to ensure that it is not a fragment of a larger agglomerate. This is done by gradually increasing the vapor

pressure in the pick-up cell and monitoring the mass spectrum for the appearance of molecular ions characteristic of progressively larger entities. For example, monomer ionization produces a strong $(DMSO)^+$ signal[28] at m=78 Da, hence if we measure beam profiles with the mass spectrometer set to this mass peak but with the vapor pressure low enough to suppress the corresponding characteristic $(DMSO)_2^+$ peak at m=156 Da, then we can be confident that the deflection principally corresponds to droplets carrying the monomer. Similarly, profiles measured at m=156 Da but before the appearance of the trimer's signal must derive from the dimer, etc. Representative mass spectra are shown in the Supporting Information (SI).

Fig. 1 shows the deflection profiles of helium nanodroplets containing one, two, and three DMSO molecules. The deflections are substantial despite the fact that the droplets are truly massive ($\sim 1\times10^4$–3×10^4 He atoms, as described in the caption). Therefore we are immediately and directly informed by Fig. 1(b) that $(DMSO)_2$ settles into a strongly polar configuration and not into its global minimum structure, because the latter would be symmetric with a zero dipole moment.[29]

In order to assign an absolute value of the dipole moment to the dopant, we must keep in mind that the host nanodroplets are not all of the same size. The size distribution produced by the nozzle expansion is log-normal, and this translates into a convolution of pick-up cross sections, deflection angles, and ionization efficiencies. Our procedure[16,17] is to start with the profile corresponding to a single DMSO dopant molecule whose dipole moment is known. A fit to the deflected profile (by a Monte Carlo simulation of the pick-up, evaporation, deflection, and detection steps) is used to calibrate the droplet size distribution. Then by repeating the deflection measurement and its simulation with doubly- and triply-doped nanodroplets produced and detected under the same conditions, we can deduce the electric dipole moments corresponding to the dimer and the trimer.

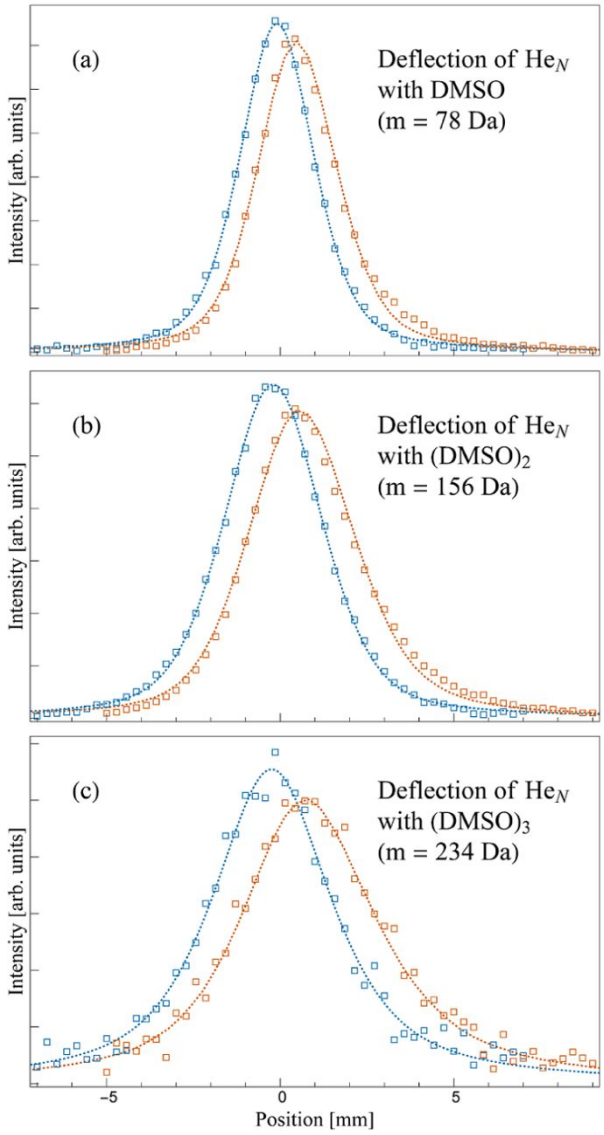

Fig. 1. Profiles of $(DMSO)_n$-doped helium nanodroplet beams. Blue: zero-field profiles, orange: deflection by a field of 82 kV/cm strength and 338 kV/cm^2 gradient. Symbols: experimental data, lines: fits of the deflection process, as described in the text. The monomer profile mapped for a particular temperature T and stagnation pressure P of the He_N beam source is used to determine the average $\bar{N}$ and width ΔN of the nanodroplet size distribution, and then fits to the dimer and trimer profiles for the same source conditions yield these dopants' dipole moments. In (a) and (b) P=80 bar, T=15.5 K, $\bar{N} \approx 2.3\times10^4$, in (c) P=80 bar, T=16.4 K, $\bar{N} \approx 1.4\times10^4$. The gradual increase of the profile width with the number of dopant molecules is caused by transverse momentum transfer associated with each pick-up collision.

These dipole moments enter the fitting procedure at the step where the deflecting electrostatic force is calculated. As described in the Introduction, this requires knowing $\overline{p}_z$, i.e., the degree of orientation induced by the applied field. For the DMSO monomer this is carried out by diagonalizing the rotational Stark effect matrix (cf. ref 30) using the components of the molecule's dipole moment.[24] For the heavier dimer and trimer the classical Langevin-Debye formula is sufficiently accurate.[31] In calculating the monomer's Stark spectra one should keep in mind that rotational coupling to the superfluid[32] enhances the moments of inertia of the heavier molecular rotors by an average factor of ~2.5-3 compared with their gas phase value.[5,18] Since DMSO's specific renormalization factor is not known, it was set to 2.6 in our data fitting procedure. We found that the inclusion of this factor had practically no effect on the deduced dipole of the dimer but shifted that of the trimer upward by ≈10%-15%. For the final fitted dipole values listed below, the $(DMSO)_n$ orientations within an applied 82 kV/cm field were found to be 86%, 97%, and 98% for n=1-3, respectively.

2.2 Dipole moments. From analysis of the measurements, we assign effective electric dipole moments of 7.2 D to $(DMSO)_2$ and 8.6 D to $(DMSO)_3$, with an estimated accuracy of ±0.2 D and ±0.6 D, respectively. These values, which can be compared with the ground state moments of 0 D for the aforementioned symmetric dimer and 4.2 D for the trimer[29] (essentially a nonpolar dimer plus an unpaired monomer), establish the presence of highly polar metastable structures. In the cold superfluid environment these structures are steered into formation by the long-range intermolecular forces and are then unable to overcome the potential barrier leading to the global minimum configuration.

2.3 Modeling of molecular complex formation. To facilitate the interpretation of the above results, we supplemented the experiments with *ab initio* modeling of DMSO

condensation. We optimized the geometry of DMSO dimers and trimers with the B3LYP functional with the aug-cc-pVDZ basis set. The DMSO complexes are dominantly bound by electrostatic forces but the dispersion interactions still play a non-negligible role. We have therefore used the D2 correction of Grimme.[33] The approach was tested against the CCSD(T)/aug-cc-pVTZ method for the DMSO dimer, yielding similar energetics (see the SI). All calculations were performed in the gas phase: by considering complexes with helium atoms or within a dielectric continuum we found that the helium environment had a negligible effect on the structure and energetics. The potential energy surfaces (PES) were pre-screened with molecular mechanics (MM)-based metadynamics simulations[34] and the structures were then recalculated at the DFT level (see the SI for further information).

The process of DMSO dimer formation was modeled with molecular dynamics (MD) simulations within the canonical ensemble. We used the Nosé-Hoover thermostat with a rather small value of $\tau = 0.01$ ps. This corresponds to fast draining of extra energy from the system, so that at each time it essentially remains in equilibrium. A temperature of 5 K was chosen in order to accelerate the simulations. It is higher than in the experiment but the difference is small compared with the PES accuracy.

We started with two DMSO molecules positioned at a distance of 20 Å between the two sulphur atoms with a random orientation. We then performed molecular mechanics simulations with the MM force field.[35] The molecules gradually approached each other while aligning their dipole moment. Since the MM force field does not reproduce the energetics of the minima sufficiently well, at the intermolecular distance of 10 Å we reset the simulations, switching from the force field to the more accurate semiempirical density functional tight binding (DFTB) method[36] with D3 dispersion correction.[37,38] The system then continued to evolve in time for another 500 ps with a time step of 1 fs, using the velocity Verlet integrator.

Dipoles along the path were recalculated at the B3LYP/aug-cc-pVDZ level.

The DFT and CCSD(T) calculations were performed in Gaussian09.[39] Molecular dynamics simulations were performed in GROMACS 2018.4[40] and the DFTB simulations in the DFTB+ 18.2 code.[36] We also utilized our in-house MD code ABIN.[41]

2.4 Results of modeling. Fig. 2 shows several low-lying minima of the DMSO dimer obtained from extensive mapping of its potential energy surface. The structures are divided into two classes of minima: non-polar and polar. The global minimum (complex D1) of $(DMSO)_2$ has a symmetrical configuration with a zero dipole moment, consistent with the aforementioned work.[29] Structures D2 and D3 also belong to the low dipole manifold. Complexes D4 and D5 represent polar type structures. The experimental data suggest that the highly polar structure D5, with an almost orthogonal arrangement of dipoles, predominantly forms within nanodroplets. It is separated from the global minimum by a barrier of 0.08 eV (see the SI), which is more than sufficient to prevent a D5 → D1 transition.

Structure formation under cryogenic conditions is therefore likely to proceed as follows. At large separation the dominant force is the dipole-dipole interaction which aligns the two DMSO molecules. As described in the SI, there is a barrierless pathway between this structure and the D5 minimum. Therefore the molecules approach each other gradually within the helium environment to which all excess energy is almost immediately drained. The $(DMSO)_2$ ends up trapped within the basin of complex D5.

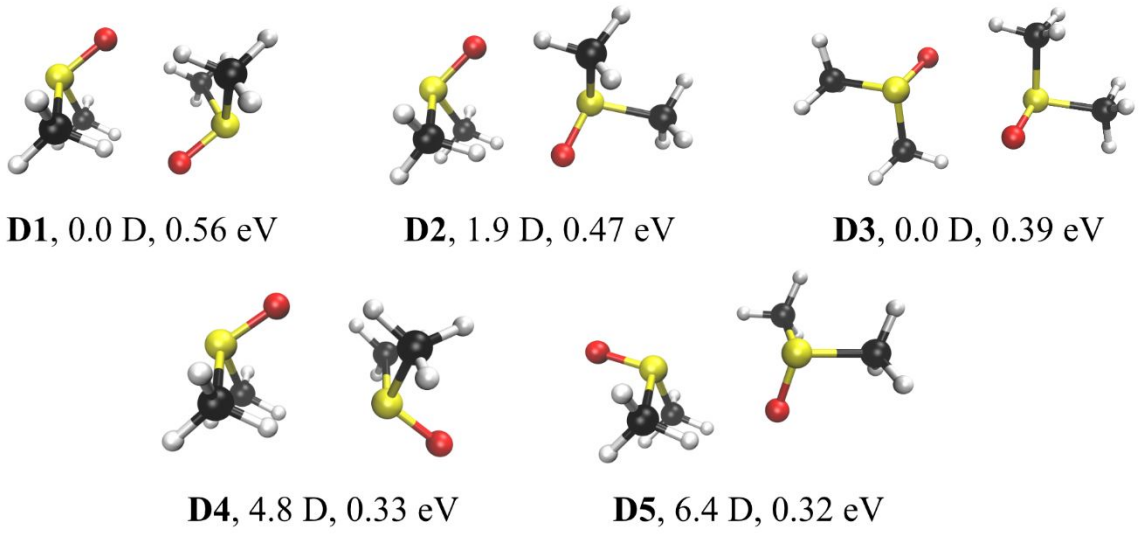

Fig. 2. Energy minima of the DMSO dimer, with their corresponding binding energies and dipole moments.

We support this scenario by molecular dynamics (MD) simulations of the binary encounter under conditions of very efficient energy transfer to the environment, as specified above. At the start the two dipoles are assigned a random relative orientation, but the trajectory shown in Fig. 3 demonstrates that it becomes correlated already at large distances. At closer approach the total dipole moment transiently increases. The molecular dipoles at that point are still parallel, hence the bump in the dipole moment is caused by mutual induction. Finally, the dimer quenches into one of the potential minima. In accord with the experiment, no formation of a zero dipole structure is found. The majority of the trajectories end up in the D5 minimum with a dipole of 6.4 D, some of them end up in the D4 minimum with a somewhat lower dipole moment than detected in the experiment. The formation of other

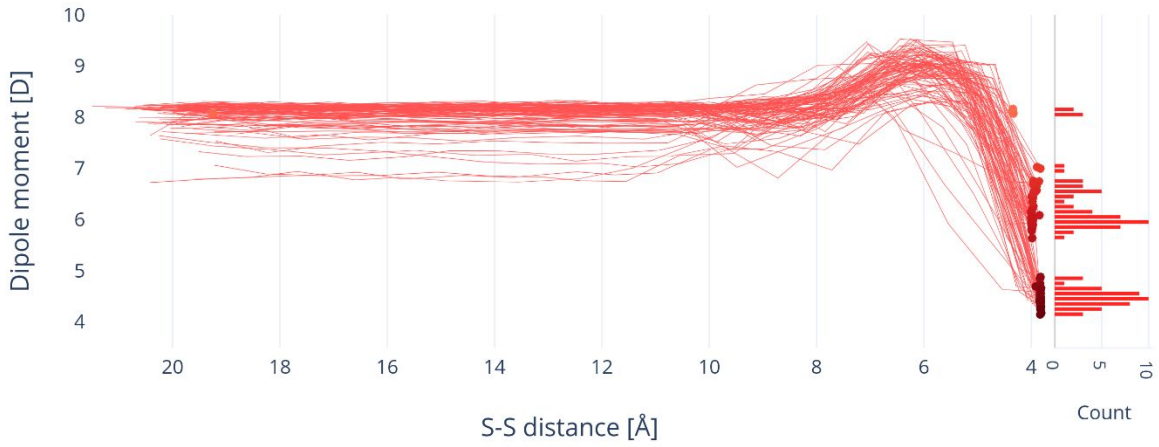

Fig. 3. Dipole moment of DMSO dimer complex along the intermolecular approach coordinate, as illustrated by a molecular dynamics simulation.

The structures are more diverse for the trimer (Fig. 4). The lowest energy structure is cyclic with a dipole moment of 4.25 D (complex T1). Its formation is kinetically hindered. Indeed, as mentioned above, it represents the global dimer minimum to which the third molecule is added; since in the nanodroplets the former structure is not formed, neither will the cyclic trimer. We have located linear structures (T6, T7) with a much higher dipole close to 10 D. There are multiple other minima with intermediate dipoles. It follows from our simulations that a rather complex mixture of these metastable structures may be formed under the experimental conditions, and its precise assignment is beyond the reach of theory. The effective dipole moment of ≈8.6 D deduced from the deflection experiment represents the population average of the kinetically accessible structures.

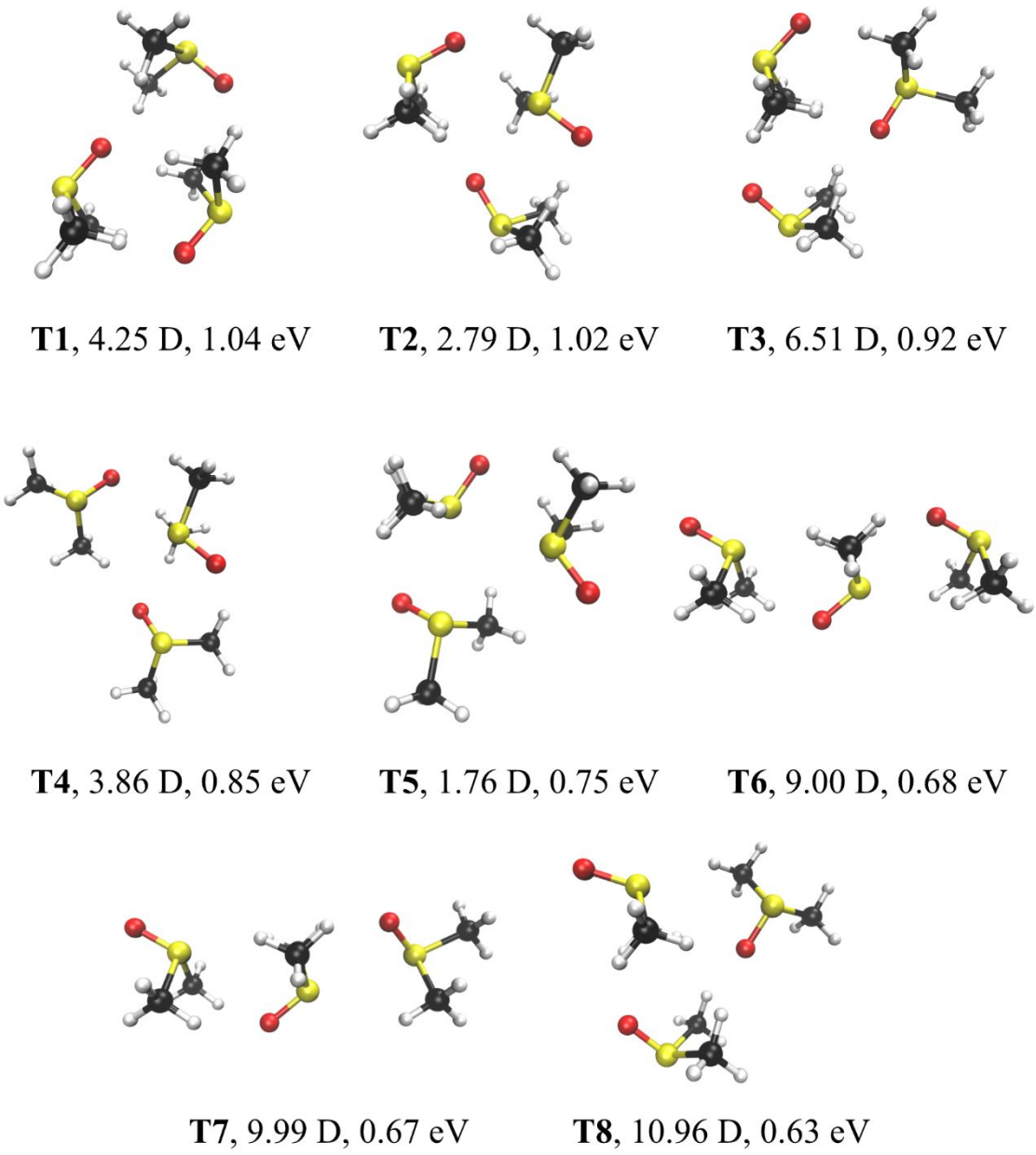

Fig. 4. Energy minima of DMSO trimers, with their corresponding binding energies and dipole moments.

3. Conclusion

In summary, we have demonstrated that the presence of peculiar polar structures, formed by sequential embedding of polar molecules into superfluid helium nanodroplets, can be clearly and directly detected by electrostatic deflection of the doped nanodroplet beam. In an application of this method to DMSO molecules we found that they form dipole-aligned dimer

and trimer structures, steered by long-range electrostatic interactions. The formation mechanism and the magnitudes of the dipole moments are in good agreement with calculations describing molecular interactions and structure formation in the viscosity-free cryogenic environment.

In future applications it will be interesting to extend this approach, for example, to a study of interactions between polar amino acids or between prototype solute and solvent molecules, as well as between molecules in photoinduced polar conformations. It is also interesting to inquire whether transfer of angular momentum between the impurities and the quantum-fluid bath, a phenomenon predicted to have the potential to screen the impurity – electric field interaction,[42] may be able to measurably affect the dynamics of molecular assembly within nanodroplets.

Conflicts of interest

There are no conflicts to declare.

Acknowledgments

This work was supported by the U. S. National Science Foundation under Grant No. CHE-1664601. L.K. acknowledges a scholarship from the Austrian Marshall Plan Foundation and support from the Austrian Science Fund under project FWF W1259. J.S. and P.S. thank the Czech Science Foundation for support under Project number 18-16577S. J.S. is an International Max Planck Research School for Many Particle Systems in Structured Environments student. We would like to thank Jiahao Liang and Atef Sheekhoon for assistance.

References

1 M. T. Bell and T. P. Softley, *Mol. Phys.* 2009, **107**, 99-132.

2 M. Schnell and G. Meijer, *Angew. Chem. Int. Ed.* 2009, **48**, 6010-6031.

3 G. Quéméner and P. S. Julienne, *Chem. Rev.* 2012, **112**, 4949-5011.

4 N. Balakrishnan, *J. Chem. Phys.* 2016, **145**, 150901.

5 J. P. Toennies and A. F. Vilesov, *Angew. Chem. Int. Ed.* 2004, **43**, 2622-2648.

6 K. K. Lehmann and G. Scoles, *Science* 1998, **279**, 2065-2066.

7 K. Nauta and R. E. Miller, *Science.* 1999, **283**, 1895-1897.

8 K. Nauta, D. T. Moore and R. E. Miller, *Faraday Discuss.* 1999, **113**, 261-278.

9 F. Madeja, M. Havenith, K. Nauta, R. E. Miller, J. Chocholoušová and P. J. Hobza, *Chem. Phys.* 2004, **120**, 10554-10560.

10 M. Y. Choi and R. E. Miller, *J. Phys. Chem. A*. 2006, **110**, 9344-9351.

11 F. Ferreira da Silva, S. Jaksch, G. Martins, H. M. Dang, M. Dampc, S. Denifl, T. D. Märk, P. Limão-Vieira, J. Liu, S. Yang, A. M. Ellis and P. Scheier, *Phys. Chem. Chem. Phys.* 2009, **11**, 11631-11637.

12 J. A. Davies, M. W. D. Hanson-Heine, N. A. Besley, A. Shirley, J. Trowers, S. Yang and A. M. Ellis, *Phys. Chem. Chem. Phys*. 2019, **21**, 13950-13958.

13 M. Ortlieb, Ö. Birer, M. Letzner, G. W. Schwaab and M. Havenith, *J. Phys. Chem. A.* 2007, **111**, 12192-12199.

14 D. Skvortsov, R. Sliter, M. Y. Choi and A. F. Vilesov, *J. Chem. Phys*. 2007, **128**, 094308.

15 K. Nauta and R. E. Miller, *Science.* 2000, **287**, 293-295.

16 D. J. Merthe and V. V. Kresin, *J. Phys. Chem. Lett*. 2016, **7**, 4879-4883.

17 J. W. Niman, B. S. Kamerin, D. J. Merthe, L. Kranabetter and V. V. Kresin, *Phys. Rev. Lett*. 2019, **123**, 043203.

18 M. Y. Choi, G. E. Douberly, T. M. Falconer, Lewis, W. K. Lewis, C. M. Lindsay, J. M. Merritt, P. L. Stiles and R. E. Miller, *Int. Rev. Phys. Chem.* 2006, **25**, 15-75.

19 Y.-P. Chang, D. Horke, S. Trippel and J. Küpper, *Int. Rev. Phys. Chem*. 2015, **34**, 557-590.

20 M. Johny, J. Onvlee, T. Kierspel, H. Bieker, S. Trippel and J. Küpper, *Chem. Phys. Lett.* 2019, **721**, 149-152.

21 B. Friedrich and D. Herschbach, *Int. Rev. Phys. Chem.* 1996, **15**, 325-344.

22 J. Bulthuis, J. A. Becker, R. Moro and V. V. Kresin, *J. Chem. Phys.* 2008, **129**, 024101.

23 W. Feder, H. Dreizler, H. D. Rudolph and V. Typke, *Z. Naturforsch.* 1969, **24a,** 266-278.

24 M. L. Senent, S. Dalbouha, A. Cuisset and D. Sadovskii, *J. Phys. Chem. A*. 2015, **119**, 9644-9652.

25 *CRC Handbook of Chemistry and Physics*, 99th edition, ed. J. R. Rumble, CRC Press, Boca Raton, 2018.

26 D. J. Merthe, PhD thesis, University of Southern California, 2017.

27 A. Mauracher, O. Echt, A. M. Ellis, S. Yang, D. K. Bohme, J. Postler, A. Kaiser, S. Denifl and P. Scheier, *Phys. Rep*. 2018, **751**, 1-90.

28 *NIST Chemistry WebBook*, *NIST Standard Reference Database Number 69,* ed. P. J. Linstrom and W. G. Mallard, National Institute of Standards and Technology, Gaithersburg, 2018, http://webbook.nist.gov (accessed May 2019).

29 N. S. Venkataramanan, A. Suvitha and Y. Kawazoe, *J. Mol. Liq.* 2018**, 249**, 454-462.

30 Y.-P. Chang, F. Filsinger, B. G. Sartakov and J. Küpper, *Comput. Phys. Commun.* 2014, **185**, 339-349.

31 L. Pei, J. Zhang and W. Kong, *J. Chem. Phys*. 2007, **127**, 174308.

32 M. Lemeshko, *Phys. Rev. Lett.* 2017, **118**, 095301.

33 S. Grimme, *J. Comput. Chem.* 2006, **27**, 1787-1799.

34 A. Barducci, M. Bonomi and M. Parrinello, *WIREs Comput. Mol. Sci*. 2011, **1**, 826-843.

35 M. L. Strader and S. E. Feller, *J. Phys. Chem. A*. 2002, **106**, 1074-1080.

36 B. Aradi, B. Hourahine and Th. Frauenheim, *J. Phys. Chem. A.* 2007, **111**, 5678-5684.

37 S. Grimme, J. Antony, S. Ehrlich and H. Krieg, *J. Chem. Phys.* 2010, **132**, 154104.

38 S. Grimme, S. Ehrlich and L. Goerigk, *J. Comput. Chem.* 2011, **32**, 1456-1465.

39 M. J. Frisch *et al*., Gaussian 09 (Rev. D.01), Gaussian, Inc., Wallingford, CT, 2009.

40 M. J. Abraham, T. Murtola, R. Schulz, S. Páll, J. C. Smith, B. Hess and E. Lindahl, *SoftwareX.* 2015, **1-2**, 19-25.

41 *ABIN, Molecular Dynamics program*. Source code available at https://github.com/photox/abin. doi:10.5281/zenodo.1228462.

42 E. Yakaboylu and M. Lemeshko, *Phys. Rev. Lett.* 2017, **118**, 085302.

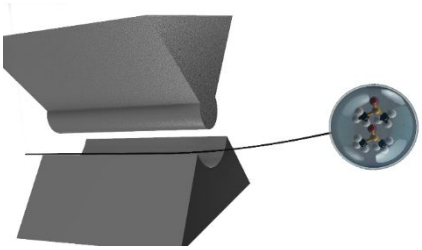

Self-assembly, via long-range forces, of highly polar molecular complexes in helium nanodroplets is revealed by electric deflection of nanodroplet beams.